UHASSELT
KNOWLEDGE IN ACTION

Maastricht University

Faculty of Medicine and Life Sciences
School for Life Sciences
Master of Biomedical Sciences

Master's thesis

DISC1 impairment disrupts cytoskeletal organization in microglia

Art Janssen

Thesis presented in fulfillment of the requirements for the degree of Master of Biomedical Sciences, specialization Molecular Mechanisms in Health and Disease

SUPERVISOR :

Prof. dr. Jelle HENDRIX

MENTOR :

Mevrouw Keerthana RAMANATHAN

2021
2022

Transnational University Limburg is a unique collaboration of two universities in two countries: the University of Hasselt and Maastricht University.

UHASSELT
KNOWLEDGE IN ACTION

www.uhasselt.be
Universiteit Hasselt
Campus Hasselt:
Martelarenlaan 42 | 3500 Hasselt
Campus Diepenbeek:
Agoralaan Gebouw D | 3590 Diepenbeek

UHASSELT
KNOWLEDGE IN ACTION

Maastricht University

Faculty of Medicine and Life Sciences
School for Life Sciences
Master of Biomedical Sciences

Master's thesis

DISC1 impairment disrupts cytoskeletal organization in microglia

Art Janssen

Thesis presented in fulfillment of the requirements for the degree of Master of Biomedical Sciences, specialization Molecular Mechanisms in Health and Disease

SUPERVISOR :

Prof. dr. Jelle HENDRIX

MENTOR :

Mevrouw Keerthana RAMANATHAN

DISC1 impairment disrupts cytoskeletal organization in microglia*

Art Janssen[1,2], Keerthana Ramanathan[2], Sofie Kessels[2], Sam Duwé[1], Yeranddy Aguiar Alpizar[2], Bert Brône[2] and Jelle Hendrix[1]

[1]Dynamic Bio-Imaging Lab, Biomedical Research Institute, Hasselt University, Campus Diepenbeek, Agoralaan building C - B-3590 Diepenbeek, Belgium
[2]Neurophysiology Lab, Biomedical Research Institute, Hasselt University, Campus Diepenbeek, Agoralaan building C - B-3590 Diepenbeek, Belgium

*Running title: *DISC1 controls microglial morphology*

To whom correspondence should be addressed: Prof. Jelle Hendrix, Tel: +32 (11) 26 92 13; Email: jelle.hendrix@uhasselt.be

Keywords: DISC1, Microglia, Cytoskeleton, Actin, Tubulin, Neurodevelopmental disorders

ABSTRACT

Neurodevelopmental disorders (NDDs) are chronic disabilities that affect the brain. Mutations in the Disrupted-in-Schizophrenia 1 (*DISC1*) gene are associated with NDDs, like schizophrenia. DISC1 is a scaffold protein with a large interactome, including many cytoskeletal proteins. The role of DISC1 in microglia, the brain's immune cells with key roles in neurodevelopmental disorders, is largely unknown. Microglial morphology, migration, and phagocytosis depend heavily on cytoskeletal proteins, including actin and tubulin. Here, we aim to discover the effects that DISC1 impairment has on the cytoskeleton of mouse microglia in order to increase the understanding of microglial function in NDDs. Using confocal microscopy *in situ*, we revealed that microglial morphology is regulated by DISC1 and that the brain environment has limited influence on this morphology. Confocal microscopy of *in vitro* samples revealed that the actin density was decreased, while the tubulin density was increased in locus impaired (LI) microglia compared to wild type (WT). Moreover, the organization and distribution of actin and tubulin was altered as well. Furthermore, structured illumination microscopy (SIM) showed that tubulin dynamics in microglia are controlled by DISC1, as LI microglia have a higher microtubule movement speed. In conclusion, the neurodevelopmental risk gene DISC1 is essential for microglial morphology, cytoskeleton organization, motility, and consequently for microglial functionality in general. However, further research is needed to reveal the exact molecular interactions between DISC1 and the cytoskeleton in microglia.

INTRODUCTION

Neurodevelopmental Disorders – Neurodevelopmental disorders (NDDs) are defined as a group of severe chronic disabilities that affect the central nervous system (CNS) and occur early in life (1). They are caused by inadequate neurological development that can lead to a wide range of symptoms, including emotional, cognitive, and motor disorders. Examples of NDDs are attention deficit hyperactivity disorder (ADHD), autism spectrum disorder (ASD), and certain mental disorders such as bipolar disorder (BD) and schizophrenia (1-3). NDDs are very common, depending on the specific type, and although they are not necessarily linked with higher mortality, they do significantly affect the quality of life of the patients and their social environment (4).

The cellular and molecular mechanisms behind NDDs are multifactorial, and the exact pathophysiology continues to elude us, however, possible mechanisms leading to NDDs have been proposed. Certain genetic causalities have been found, although there is no *Bona Fide* genetic defect responsible for specific NDDs. For example, genes associated with the phosphatidylinositol 3-

kinase (PI3K)-mTOR pathway are affected in several NDDs (5, 6). The PI3K-mTOR pathway regulates neuronal progenitor proliferation and differentiation during embryonic development. Later in life, it is associated with cognitive processes (5). Alterations to the circadian rhythm, and the CLOCK genes associated with this system, have also been linked with certain NDDs such as ADHD (7, 8). Changes in both the dopaminergic and GABAergic systems have been linked with NDDs (7, 9). Finally, the importance of maternal immune activation (MIA) has become clearer lately. The MIA hypothesis proposes that activation of the immune system during pregnancy, in response to certain exposures, can affect the neurodevelopment of the fetus and increase the vulnerability to NDDs (10-12). Possible exposures include stress, gut microbiome, diet, sleep, exercise, pollution, infection, and socioeconomic status (12). Evidence for this theory can be found in clinical observations that link acute infections during pregnancy with NDDs (13). Furthermore, autoimmune disorders, obesity, and other causes of (low-grade)-inflammation are also found to be associated with an increased risk of NDDs (12). These exposures generate pathogen-associated molecular patterns (PAMPs) or damage-associated molecular patterns (DAMPs), that are subsequently recognized by toll-like receptors (TLRs) that stimulate pro-inflammatory cytokine production by innate immune cells (12, 14). These pro-inflammatory cytokines, including interleukin (IL)-6, IL-17, tumor necrosis factor (TNF), and IL-1β, produced by the maternal immune system, can cross the placenta and reach the fetus. There these cytokines can affect neurodevelopment and disrupt synapse function. Several other molecules can have similar effects on the developing brain, such as C-reactive protein (CRP), auto-antibodies, and complement proteins (11, 12, 15). The main cytokine-releasing cells in the CNS are the microglia which are therefore important mediators of MIA.

The role of microglia in neurodevelopmental disorders – Microglia are the resident innate immune cells of the CNS, however, their functions are diverse. Microglia are hematopoietic cells, contrasting the origin of other brain-residing cells, such as neurons and astrocytes from neuroectodermal origin (16). Their lineage also differs from peripheral phagocytic immune cells, however, certain studies have shown that bone marrow-derived microglia can reside in the CNS too (16, 17). In early development, apoptosis is very common, and microglia are involved in clearing debris of these apoptotic cells. Furthermore, microglia have roles in synapse formation, maturation, and elimination through cytokine signaling and phagocytosis (18, 19). In the normal adult brain, microglial functionality consists of immune defense in the form of cytokine release and pathogen phagocytosis, maintenance of brain homeostasis by pruning excess or weak synapses, eliminating cellular debris, and scanning the brain for possible danger. In addition, microglia use cytokine signaling to stimulate neuron and synapse survival (19). During this period in life, the microglia are in a more passive resting state and are highly ramified, meaning that they have an abundance of branches, allowing the cells to scan their environment (20). When microglia are activated, their shape changes, and they become less ramified, allowing for easier migration towards regions of potential danger. Other characteristics of activated microglia include increased immunological activation and increased phagocytic ability (19). In the brains of patients with NDD, there are more activated microglia and less ramified cells (20). Similarly, more primed microglia are found in certain NDDs, probably due to environmental triggers early in life associated with MIA (20). NDDs also affect the synaptic density, which is aberrant, depending on the specific disorder. Brains of ASD patients, for example, have an excessive number of synapses, while their density in schizophrenia is decreased. These aberrations have mainly been attributed to changes in microglial gene transcription and functionality, and because there is a difference in microglial activation in NDDs, as mentioned above (21, 22). Thus, evidence indicates that microglia in NDD have different phenotypes compared to healthy microglia.

Microglial cytoskeleton dynamics as a necessity for proper microglial functioning – Essential microglial functions such as phagocytosis, migration, and ramification rely heavily on cellular movement, and therefore cytoskeletal remodeling is essential for normal microglial functionality. The cytoskeleton exists of

three main components: actin, microtubules (MTs), and intermediate filaments (IFs). The crosstalk between these components and linking molecules is essential in all movement and structure based cellular activities (23). The actin cytoskeleton consists of globular actin (G-actin) that can polymerize into filamentous actin (F-actin), with both forms being in equilibrium. Actinin is a protein that crosslinks actin fibers to strengthen the meshwork, and myosin motor proteins associate with actin as well to provide the contractile forces needed for cellular movement. MTs are hollow tubes with an outer diameter of 23-27 nm. They consist of dimers of α-tubulin and β-tubulin. The MTs provide polarity in the cell during cellular movement such as migration. Furthermore, MTs can accommodate intracellular transport of certain groups of (cytoskeletal) molecules and proteins (23, 24). Finally, there are many different IF proteins, and their functions vary significantly (23).

These cytoskeletal components can form certain structures by associating with cytoskeleton-associated proteins. Focal adhesions (FAs) are structures of proteins that connect the cell to the extracellular matrix (ECM). At the outside of the FA, in contact with the ECM, integrins can be found. Linker molecules including vinculin, talin and paxillin connect these integrins to the actin meshwork. Furthermore, these FAs give rise to stress fibers which are actomyosin fibers that span the cell body and have the ability to contract (25). The FAs are essential for migration in all cell types, including microglia, and during CNS development, (microglial) migration is crucial. During cell migration, the cell polarizes into a rear end, and a wide cell protrusion called the lamellipodium. Lamellipodia consist mainly of a polymerized actin meshwork that is highly dynamic. FAs form in the lamellipodia area, and the actomyosin stress fibers will contract with the help of Rho GTPases. This drags the cell forward, and meanwhile, the FAs in the rear end of the cell will disassemble while the microtubules transport these disassembled components to the leading end of the cell for new FA assembly (25). A second type of membrane protrusion called the filopodia is sometimes present at the leading edge, as well. These are very thin membrane protrusions initiating from the lamellipodium and consisting mainly of actin. During cell migration, the filopodia serve primarily as antennae that scan the environment (26).

Disrupted-in-Schizophrenia 1 – Due to the importance of cellular movement and migration of microglia in NDDs, the cytoskeleton and associated proteins and genes are interesting research targets. Disrupted in Schizophrenia 1 (DISC1) is such a protein that is heavily studied in the context of NDDs such as Schizophrenia, BD, ASD and major depression disorder. *DISC1* is located at 1q42.1 and was first discovered in 2000 in a Scottish family with a high incidence of mental illness. The original disruption in this family consisted of a (1;11)(q42.1,q14.3) translocation (27, 28). Later, however, more than 50 other mutations linked to NDDs have been identified, most of them located in the N-terminus part of the protein (27, 29).

DISC1 is a scaffolding protein, meaning that it is involved in many different signaling pathways, with a large interactome. DISC1 is associated with the Wnt signaling pathway, mitochondrial calcium homeostasis, CNS cell proliferation, synapse maturation, cell-ECM adhesion, mTOR signaling, neuron migration, and microtubule organization among other things(30). Most of the research on DISC1 has been done in neurons, however, DISC1 expression has been identified in microglia (31), and recently the importance in astrocytes on cognitive function has been discovered (32).

As mentioned above, DISC1 is involved in neurodevelopment through pathways such as Wnt and mTOR signaling, both essential pathways for (neuronal) cell proliferation and differentiation (33-35). Furthermore, DISC1 has known interactions with Ndel1, a cell cycle protein that has a role in CNS development, and several cytoskeletal proteins (36).

In neurons, FEZ1 has been found to interact with DISC1, a protein that can directly interact with F-actin and has functions related to axonal growth polarization. Next, DISC1 interacts with motor proteins Kinesin-1, dynein, KIF1B, implying a role in various cytoskeletal transport methods (37). Furthermore, DISC1 interacts with microtubules through proteins MIPT3 and MAP1A. Finally, DISC1 interacts with TNIK and Kalirin-7, two actin-associated proteins that are involved with spine regulation and actin depolymerization, respectively (38).

Lastly, research in T cells showed that DISC1 forms a complex with girdin, and the absence of this

complex prevented actin polymerization, a crucial part of all cellular movement (39).

DISC1 is involved with neuronal development via several pathways. One way that DISC1 hampers development is through the cytoskeleton, a subcellular component that is crucial for cellular movement. Microglia, important regulator cells of the CNS, rely on the cytoskeleton for their movement-based functions like migration and phagocytosis. There is, however, no research conducted regarding the role of NDD risk genes, including DISC1, in microglia. Therefore, we will focus on finding a link between DISC1 and microglial dynamics, as these are essential for normal brain development. Gaining a better understanding of the molecular basis of microglial motility and the influence of DISC1 could lead to the discovery of new therapeutic targets for NDDs. We hypothesize that DISC1 LI microglia have an altered morphology, cytoskeleton structure, and tubulin dynamics compared to WT microglia.

In this study, we used confocal imaging to study the microglial morphology of brain slices from DISC1 locus impaired (LI) mice compared to wild type (WT). Next, we used Airyscan microscopy and immunostaining to investigate the structure of the actin and tubulin cytoskeleton in DISC1 WT and LI primary mouse microglia. Finally, we used a super-resolution microscopy technique called structured illumination microscopy (SIM) to study the dynamics of the tubulin cytoskeleton in DISC1 WT and LI microglia in mice. These experiments allowed us to examine the effect of DISC1 locus impairment on the cytoskeleton of microglia in mice.

EXPERIMENTAL PROCEDURES

Animal model – A DISC1 LI mouse model, designed by Prof. Dr. Sawa and colleagues at the John Hopkins University (Baltimore, USA), was used (40). The model lacks the two most important DISC1 isoforms because of 40 kilobase pairs (kbp) exclusions in exon 1-3, Tsnax/Trax-Disc1 intergenic splicing, and a microRNA in intron 1. Furthermore, a 25 bp loss in exon six can be found. $DISC^{+/LI}$ (HET) mice were bred to obtain both $DISC1^{+/+}$ (WT) and $DISC1^{LI/LI}$ (LI) pups. The pups were sacrificed around one to three days (P1-3) for microglia isolation.

Next, a bone marrow transfer (BMT) mouse model was designed to examine migrating microglia-like cells from the bone marrow to the brain. 10-weeks old *Disc1*$^{WT/WT}$ and *Disc1*$^{LI/LI}$ were anesthetized intraperitoneally with ketamine (30 mg/kg) and xylazine (5 mg/kg) diluted in sterile phosphate-buffered saline (PBS). The anesthetized mice were irradiated with a lethal dose of 8 grays of gamma radiation and were immediately intravenously injected with 5×10^6 bone marrow cells dissolved in sterile PBS. The bone marrow cells were harvested from the femurs and tibia of 6 weeks-old gender-matched *Disc1*$^{WT/WT}$ *Cx3cr1*$^{eGFP/+}$ and *Disc1*$^{LI/LI}$ *Cx3cr1*$^{eGFP/+}$ mice. Filtered tap water, supplemented with Neomycin (100mg/l, Gibco, USA) and Polymyxin B sulfate (60 000 U/l), Sigma-Aldrich, USA) was administered to the mice two weeks before and four weeks after irradiation, and the animals were monitored daily for the first ten days post-irradiation. One week after BMT, the mice received chow containing colony-stimulation factor 1 receptor (CSF1R) inhibitor PLX5622 (1200 mg/kg standard chow, Chemgood, USA) for two weeks. CSF1R is necessary for microglia survival, and PLX5622 inhibition eliminates viable microglia, allowing for an increased repopulation of the brain with microglia-like cells from the donor bone marrow. Imaging experiments were conducted 13 weeks after BMT.

Mouse genotyping – The KAPA mouse genotyping kit (Hoffman – La Roche, Switzerland) was used for DNA extraction from the tails or toes of the mice. The samples were heated to 75°C for 10 minutes, followed by 5 at 95°C. Afterward, the polymerase chain reaction (PCR) mix, containing the DISC1 or CX3CR1-eGFP (10 µM; Integrated DNA technologies, USA) was added. The PCR process included: one cycle of 3 min at 95°C; 35 cycles of (1) 15 sec at 95°C, (2) 15 sec at 54°C, and (3) 30 sec at 72°C, and finally, another cycle of 3 min at 72°C.

The CX3CR1-eGFP genotyping required a touchdown PCR, where the annealing temperature was reduced by 0,2% each cycle. Here, the PCR process included: one cycle of 3 min at 95°C; 35 cycles of (1) 30 sec at 94°C, (2) 15 sec at 64-58°C, and (3) 1 min at 72°C; one cycle of 7 min at 72°C. The primers used for genotyping were as follows: *Disc1* fwd 5'- GCTGTGACCTGATGGCACT-3', *Disc1* rev 5'-GCAAAGTCACCTCAATAACCA-3', *Cx3cr1*$^{+/+}$ fwd 5'-GTCTTCACGTTCGGTCTGGT-3', *Cx3cr1*$^{eGFP/eGFP}$ fwd 5'-

CTCCCCCTGAACCTGAAAC-3', *Cx3cr1* rev 5'-CCCAGACACTCGTTGTCCTT-3'.

The 3% agarose gel with 1% GelRed (Thermo Fischer Scientific, USA) was loaded with the samples and Smart ladder (Eurogentec, Belgium). A voltage of 150V was used to execute the gel electrophoresis, and the bands were analyzed with UV imaging. Amplicons were expected at 196 bp (*Disc1*$^{WT/WT}$), 171 bp (*Disc1*$^{LI/LI}$), 500 bp (*Cx3cr1*$^{eGFP/eGFP}$) and 410 bp (*Cx3cr1*$^{+/+}$).

Microglia isolation – P1-3 pups were decapitated before brain isolation. Meninges and the cerebellum were removed, and the brain was dissolved in Dulbecco's Modified Eagle Medium (DMEM; D5796, Sigma-Aldrich, USA) supplemented with 10% Fetal Bovine Serum, 10% Horse Serum, and 1% Penicillin/Streptomycin (Sigma-Aldrich, USA), named DMEM 10.10.1. The cells were kept in Poly-D Lysine (PDL) (20µg/ml, Gibco, Thermo Fischer Scientific, USA) pre-coated T75 culture flasks (Greiner, Austria) in the CO_2 incubator (5% CO_2, 37°C) for two weeks. The medium was refreshed after 5-7 days and supplemented with 30% colony stimulating factor 1-conditioned medium from cultured L929 cells, in order to improve the microglial growth. After two weeks, the microglia were isolated from the other glial cells with the use of the orbital shaker (3h, 6g at 37°C), and they were seeded (10^5 cells/well) on coverslips or µ-Slide 8 well plates (Ibidi, Germany) coated with PDL (20µg/ml) with DMEM 10.10.1.

Microglia morphology – The BMT mice were anesthetized 9 weeks after the BMT with 20% dolethal (Vibrac AH, USA) diluted in 0.4% heparin-PBS solution (LEO Pharma, Denmark). The mice were first transcardially perfused with PBS-heparin and afterward with 4% paraformaldehyde (Thermo Fisher Scientific, USA) enriched with 0.002% heparin. After brain isolation, slices of 100 µm were obtained with the use of the vibrating HM650 V microtome (Thermo Fisher Scientific, USA). Brain slices were mounted on glass coverslips and imaged with the Plan-ApoChromat 63×/1.40 Oil DIC M27 objective of the Zeiss LSM880 microscope (Carl Zeiss AG, Germany). The slices were excited with the CW Argon Laser at 488 nm, and Z-stacks containing 20 slices were made. Analysis of the morphology of the microglia included cropping out the cell in 3D in FIJI (ImageJ, USA) in order to determine the cellular skeleton with the Vaa3D software. This skeleton was analyzed using the sholl analysis and MATLAB software.

Immunostaining – Primary microglia were fixated with 4% paraformaldehyde for 15 min at room temperature (RT). The cells were washed with washing buffer (0.2% Triton X-100 in 1X PBS) 3 times for 5 min. Afterward, the cells were incubated with a blocking buffer with sucrose (0.2% Triton X-100, 0.3% Tween-20, 5% bovine serum albumin (BSA), and 5% sucrose in 1X PBS) for one hour at RT. The primary antibody against β-tubulin (1:1000, St Johns Laboratory, UK) was incubated at 4°C overnight in a blocking buffer without sucrose (0.2% Triton X-100, 0.3% Tween-20, 5% BSA in 1X PBS). The cells were washed with washing buffer and incubated for one hour at RT with the secondary antibody, goat anti-rabbit Alexa Fluor 555 (1:1000 Thermo Fisher Scientific, USA), and Alexa Fluor 647-Phalloidin (1:40 Thermo Fisher Scientific, USA). The cells were washed, incubated with DAPI (1:10 000) for 15 min at RT, and mounted onto glass slides with fluoromount-G (Thermo Fisher Scientific, USA). Imaging was done with the Plan-ApoChromat 63×/1.40 Oil DIC M27 objective of the Zeiss LSM880 microscope (Carl Zeiss AG, Germany) and the Airyscan detector. A Z-stack was obtained for each cell, and analysis was done with FIJI and ImageJ plugins, including the Actin Distribution Quantification (41).

Structured illumination microscopy (SIM) – Microglia, seeded on a µ-Slide 8 well plate (Ibidi, Germany), were stained with SPY555-tubulin (Spirochrome, Switzerland) in a 1:1000 dilution. Zeiss Elyra PS.1 (Carl Zeiss AG, Germany) was used with the Plan-ApoChromat 63×/1.40 Oil DIC M27 objective for the SIM imaging with an excitation at 561 nm. Sixty images were made per cell with a time interval between images of 5 seconds. The images were analyzed with the PIVlab app (42) designed for MATLAB.

Statistics – The results were analyzed with GraphPad Prism 9. Error bars represent the standard deviation (SD) unless stated otherwise. Distributions were tested for normality (Shapiro-Wilk test) and parametric or non-parametric two-tailed tests were applied accordingly. Specific information for each statistical analysis is provided in the figure legends. P values < 0.05 were considered significant and are represented by *, p

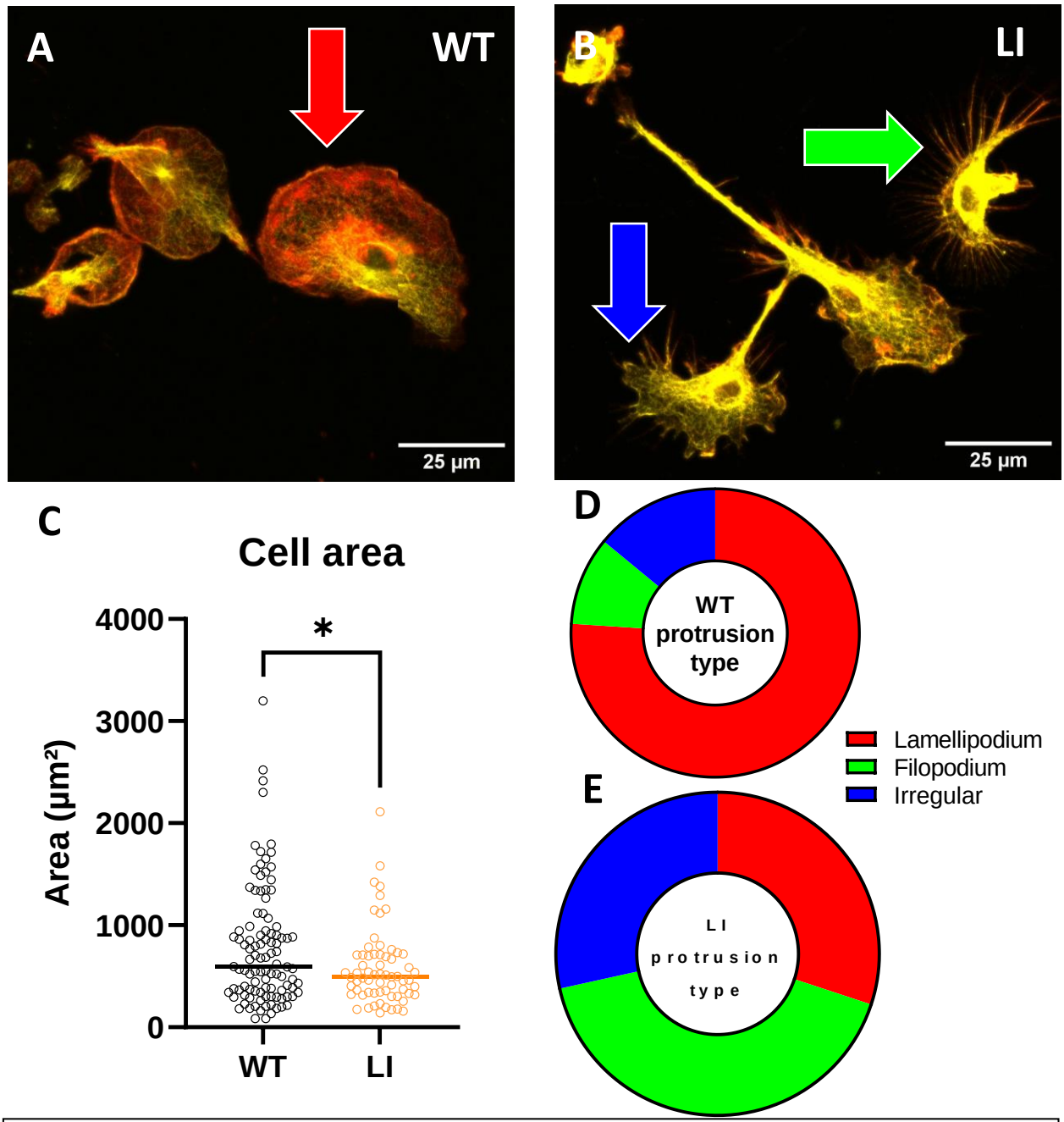

Figure 1: Cell area and shape are disrupted in DISC1 LI microglia. (A-B) Representative merged overview images of *in vitro* (A) WT and (B) DISC1 LI microglia stained with a β-tubulin antibody (Yellow) and Phalloidin-AF647 (Red) (Scale bar is 25 µm as indicated). **(C)** Cell area of WT microglia (n = 103) compared to DISC1 LI (n = 65). The horizontal bars represent the median. *p < 0.05; unpaired two-tailed Mann-Witney test. **(D-E)** Proportion of different protrusion types in (D) WT microglia compared to (E) DISC1 LI microglia, divided in three different types: large round lamellipodia; small spikey filopodia and other/irregular shapes. Arrows indicate an example per different protrusion type.

values < 0.01 are depicted with **, p < 0.001 is annotated by ***, and finally, **** represents p < 0.0001.

RESULTS

DISC1 regulates microglia morphology – The morphology of microglia is a good indication of their functionality. For example, ramified microglia

are passive and scan the environment for threats, while rounded cells without ramifications are activated microglia (20). For the purpose of studying the effect of DISC1 on the morphology of microglia, we first explored the differences in size between WT and DISC1 LI mice microglia *in vitro*. Confocal images of microglia stained for β-tubulin and F-actin were used (Figure 1A-B). The total cell area was determined (Figure 1C). WT microglia were significantly larger in size, with a median area of 593,9 $\mu m^{2,}$ while DISC1 LI microglia had a median area of 494.6 μm^2 ($p = 0.0409$). This result indicates that DISC1 LI cells are smaller and that DISC1 plays a role in obtaining a normal cell size. Next, we examined the type of protrusions that were present in microglia. The protrusions of microglia can vary from cell to cell. Lamellipodia are wide, rounded protrusions, while filopodia possess a very small, spiked shape. The majority of WT protrusions consisted of lamellipodia (76%),

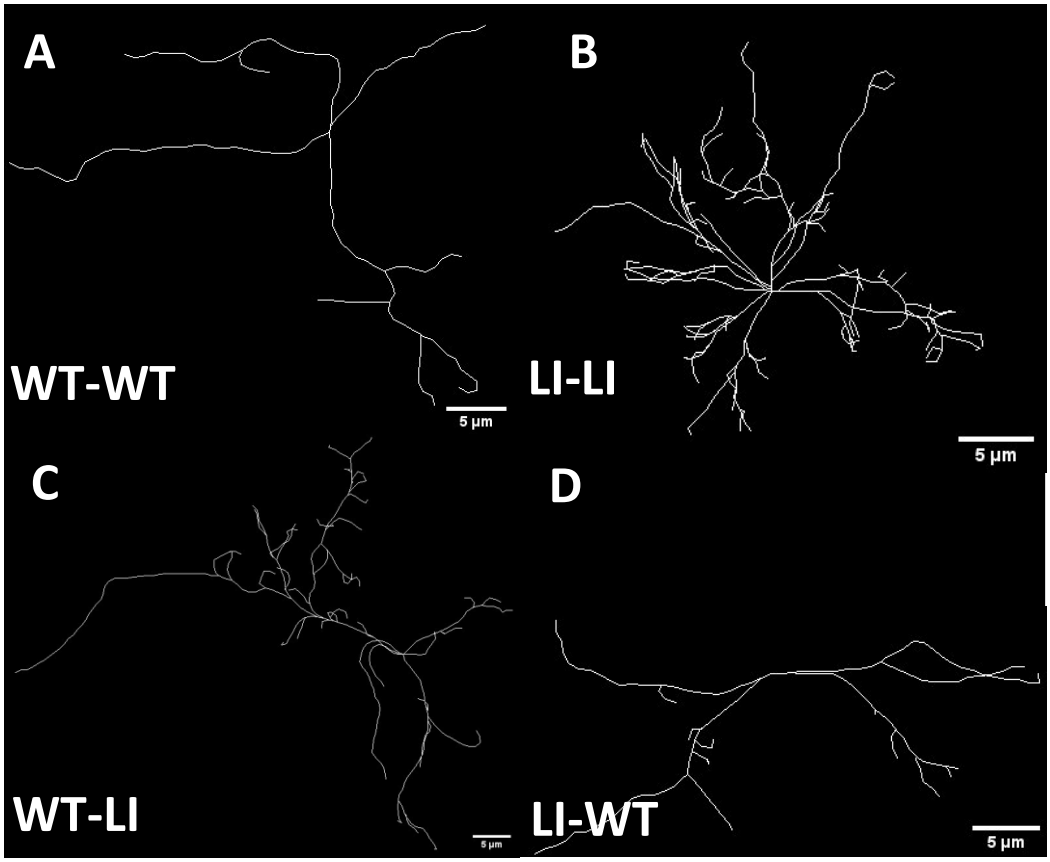

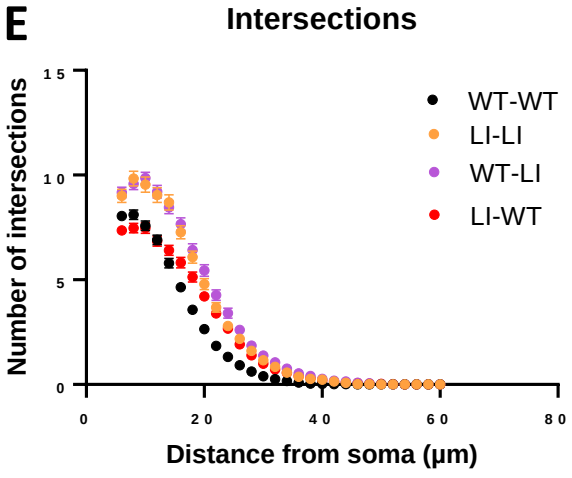

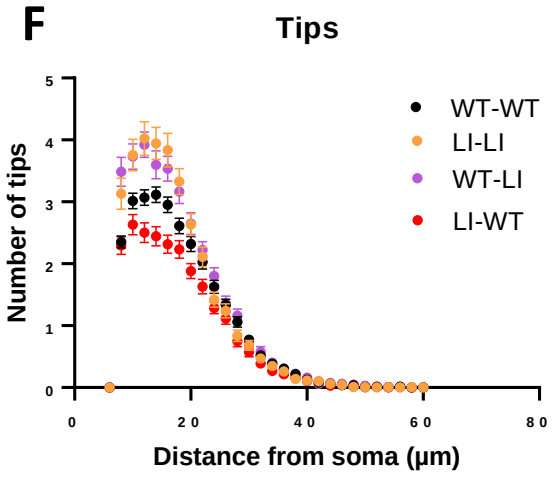

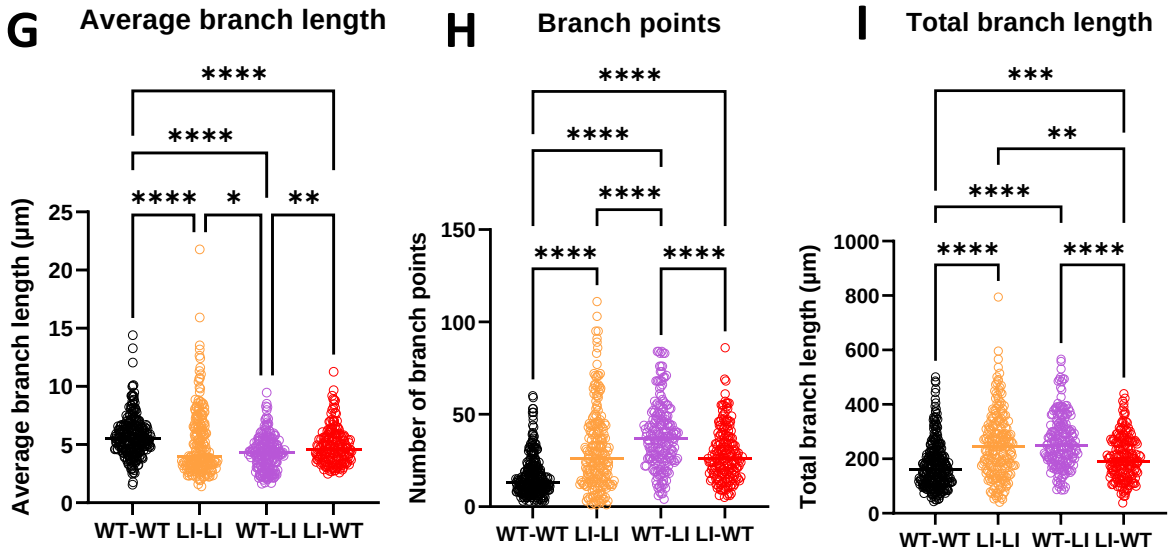

Figure 2: Morphology of DISC1 LI microglia is genotype-dependent. (A-D) Representative skeletonized cells of BMT microglia including **(A)** WT acceptor with WT bone marrow transplantation, **(B)** LI acceptor with LI donor marrow, **(C)** WT acceptor that received LI donor marrow, and finally **(D)** LI acceptor receiving WT marrow. Sholl analysis showing the **(E)** amount of intersections and **(F)** amount of tips for each radius from the soma of the cell. **(G)** Average branch length, **(H)** number of branch points and **(I)** total branch length for all 4 genotypes. $n_{WT-WT} = 280$, $n_{LI-LI} = 212$, $n_{WT-LI} = 194$, $n_{LI-WT} = 185$, all from 6 different animals with 3 males and 3 females. The horizontal bar represents the mean. The error bars in E+F represent the SEM. The Kruskall-Wallis test was performed in G-I. *p < 0.05, **p < 0.01, ***p < 0.001, ****p < 0.0001.

with only a small portion of filopodia (10%) and irregular protrusions (14%) (Figure 1D). Every protrusion that was not thin and spiked (filopodium), or big and round with an actin border (lamellipodium), was classified as an irregular protrusion. The cellular shape of DISC1 LI microglia, on the other hand, consisted mostly of filopodia (41%) but the other types were also decently represented with 30% of lamellipodia and 28% of irregular protrusions (Figure 1E). These results indicate that DISC1 LI microglia have less consistent types of protrusions. Lamellipodia are seen in migrating microglia as they allow them to move their cell body. This means that the migration of LI microglia could be impaired.

The morphology of microglia *in vitro* may, however, differ significantly from the *in situ* morphology as there are external stimuli and an extra dimension that can influence the morphology. Moreover, DISC1 is widely known to affect neurons, and the environment of microglia could affect the morphology as well. Therefore, a BMT experiment in mice was designed, where native microglia are eliminated, and bone marrow is transplanted, causing microglia-like cells to migrate to the brain. These cells are genetically modified to express eGFP and were later skeletonized (Figure 2A-D). This skeleton was used to analyze the microglial morphology with sholl analysis. The sholl analysis determines the amount of branches in a certain radius from the middle of the cell. This parameter is called intersections (Figure 2D). The sholl analysis did not reveal striking differences between DISC1 LI microglia-like cells in a DISC1 WT or DISC1 LI environment. Only at 20 and 24 µm from the soma, statistical differences ($p < 0.05$) can be found. Microglia of $Disc1^{WT/WT}$ recipients of $Disc1^{WT/WT}$ bone marrow (WT-WT) are also relatively similar to microglia of $Disc1^{LI/LI}$ recipients of $Disc1^{WT/WT}$ bone marrow (LI-WT), but mostly at shorter distances from the soma (ns at 10 and 12 µm from soma and $p < 0.05$ at 6, 8 and 14 µm). Meanwhile, the other conditions including $Disc1^{LI/LI}$ recipients of $Disc1^{LI/LI}$ bone marrow (LI-LI) and $Disc1^{WT/WT}$ recipients of $Disc1^{LI/LI}$ bone marrow (WT-LI), have significantly

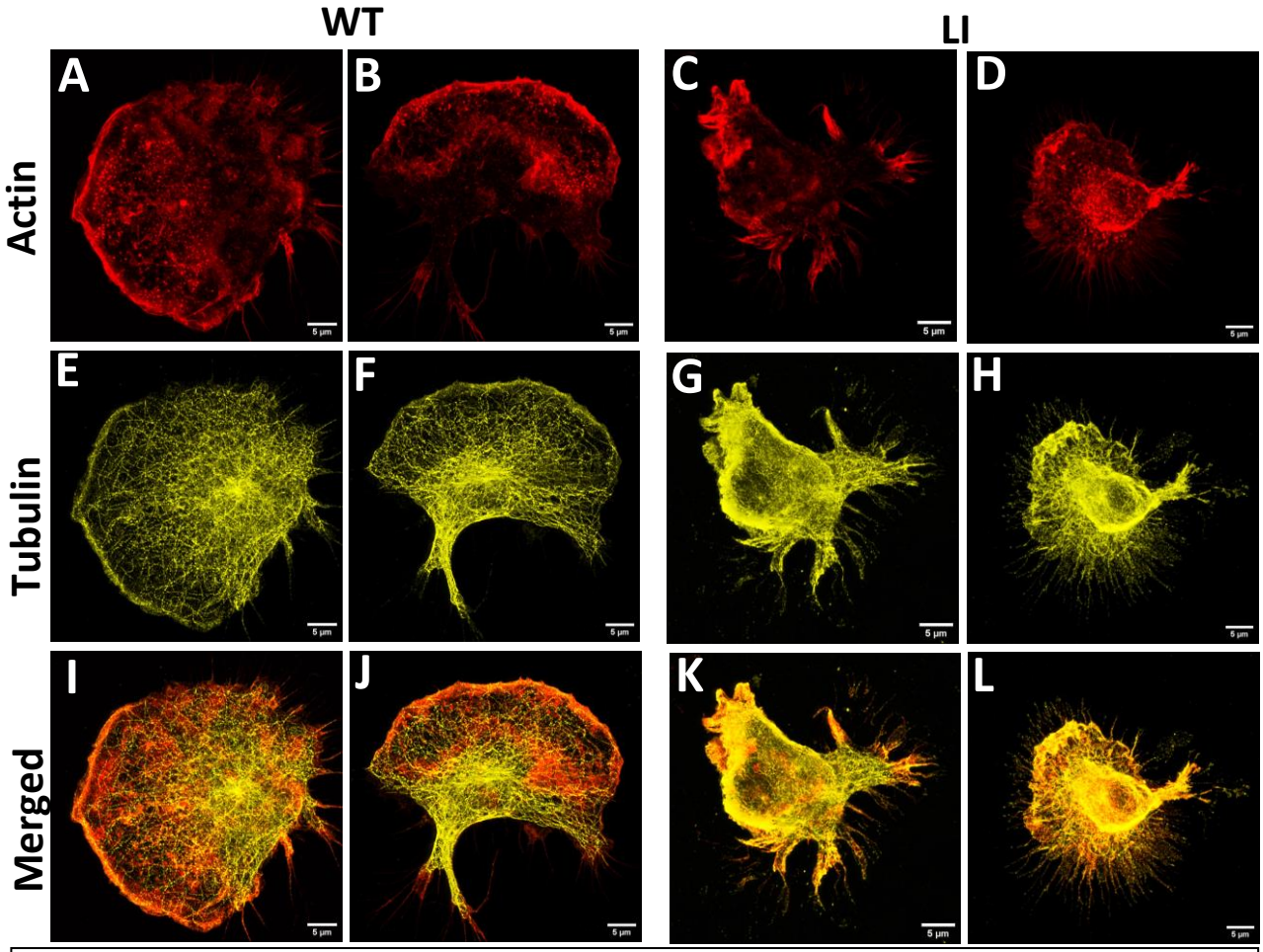

Figure 3: Representative immunofluorescence stainings of actin and tubulin in WT and DISC1 LI microglia. (A-D) Phalloidin-AF647 stained (A-B) WT and (C-D) DISC1 LI microglia show actin in red. **(E-H)** β-tubulin antibody stained (E-F) WT and (G-H) DISC1 LI microglia show tubulin in yellow. (**I-L)** Actin and tubulin channels are merged. Scale bar is 5 µm.

more intersections from 6 to 32 µm from the soma ($p < 0.05$). At longer distances from the soma, the amount of intersections seems to be closer between genotypes, although WT-WT only converges with the other genotypes at around 34 µm (See Supplementary Table 1 for a full overview of all p-values). These results demonstrate that the grade of ramification is mostly dependent on the donor genotype. However, there are still differences between the same donor types, implying that the environment might influence the morphology as well, although less pronounced than the genotype effect. These results also reveal that the changes in morphology can be found mostly in the shorter ranges rather than the larger ones.

Besides the number of intersections, the number of tips for each radius can be calculated with the sholl analysis as well (Figure 2E). Here we can see roughly the same trend as seen in the intersections. LI-LI microglia have significantly more tips from 8 to 18 µm from the soma than WT-WT microglia ($p < 0.0001$). LI-WT microglia have fewer tips from 10 to 22 µm from the soma, while WT-LI has significantly more tips from 8 to 18 µm ($p < 0.05$). Furthermore, LI-LI and WT-LI microglia tip numbers are not significantly different from each other (all p-values will be represented in Supplementary Table 2). The conclusion of this analysis is mostly the same as that of the intersections, meaning that the donor genotype has the biggest influence on the phenotype of the cell.

In Figure 2G, the average branch length per genotype is shown. The highest average branch length belongs to the WT-WT category with

5,711 µm (LI-LI = 5.171 µm; WT-L I= 4.273 µm; LI-WT = 4.868 µm). The average branch length of this genotype is significantly different from all other genotypes ($p < 0.0001$). The other genotypes are more similar, but there are still significant differences between LI-LI and WT-LI ($p = 0.0199$) and WT-LI and LI-WT ($p = 0.0084$). These results suggest that the average branch length is mainly regulated by the donor genotype, but the effect is smaller than that seen in the tips and intersections of the sholl analysis. The mean number of branch points for each genotype is depicted in Figure 2H. Here we see that the WT-LI microglia have the highest mean number of branch points with 38.3 (WT-WT = 16.3; LI-LI = 31.0; LI-WT = 28.5). All conditions are significantly different from each other ($p < 0.0001$) except LI-LI and LI-WT. Finally, the total branch length shown in Figure 2I is higher in LI donor conditions (LI-LI = 249.4 µm; WT-LI = 264.7 µm), while the WT donor genotypes have the lowest total branch length (WT-WT = 177.1 µm; LI-WT = 205.6 µm). All conditions are significantly different from each other ($p < 0.01$) except LI-LI and WT-LI.

From these experiments, we can conclude that DISC1 LI microglia have an altered morphology and that the morphology is mainly dependent on the microglial genotype rather than the environmental genotype.

Microglial actin and tubulin cytoskeleton is altered by DISC1 locus impairment – In order to examine the effect that DISC1 has on the actin and tubulin cytoskeleton, we used the Airyscan detector to make high resolution and high brightness images of immunostained WT and DISC1 LI primary microglia (Figure 3). Some differences are clearly visible when observing the confocal images. First, the WT microglia have a much more regular cell shape that is more rounded than the DISC1 LI counterpart. This observation is in line with the conclusions of the experiment shown in Figure 1 D+E, where we saw that the protrusions were very different in both genotypes. In the actin channel (Figure 3 A-D), we see that the WT microglia have a round border of actin, resulting from the presence of the lamellipodium. In the LI actin channel, we see a less organized actin distribution. The total actin density of WT microglia seems to be higher as well. Further, it seems like there are more FAs in the WT microglia compared to the LI cells (FAs can be seen as little round points in the actin channel). The tubulin distribution (Figure 3E-F) in LI microglia appears to be much denser than the WT counterpart, where the individual microtubule fibers are clearly visible.

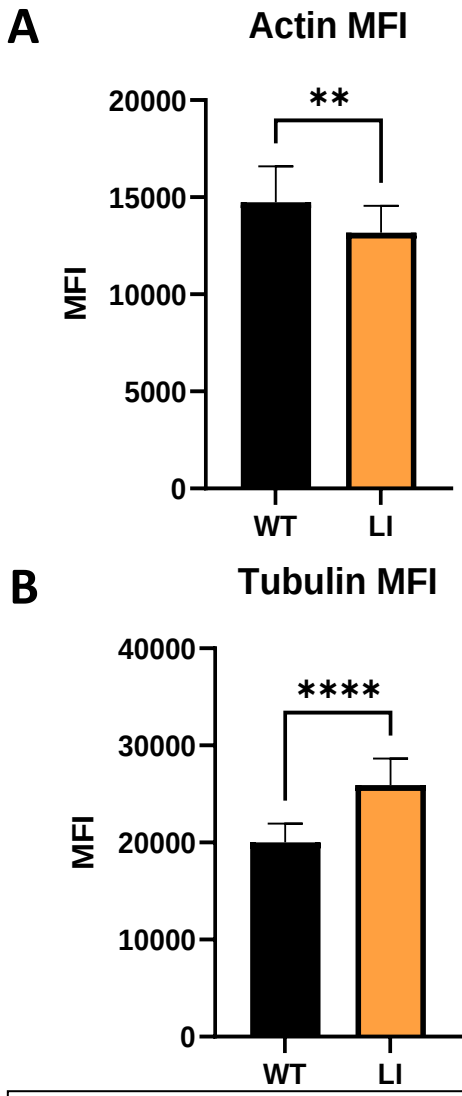

Figure 4: DISC1 LI microglia have different actin and tubulin densities compared to WT microglia. Mean fluorescence intensity (MFI) was determined for all cells for both the **(A)** actin channel and the **(B)** tubulin channel. Error bars represent the SD. MFI has AU as unit. (A) uses the Mann-Whitney test, (**$p = 0.0073$) while (B) uses an unpaired t-test (****$p < 0.0001$). N = 15 cells per genotype.

To confirm if the actin and tubulin density was defined by the genotype of microglia, the mean

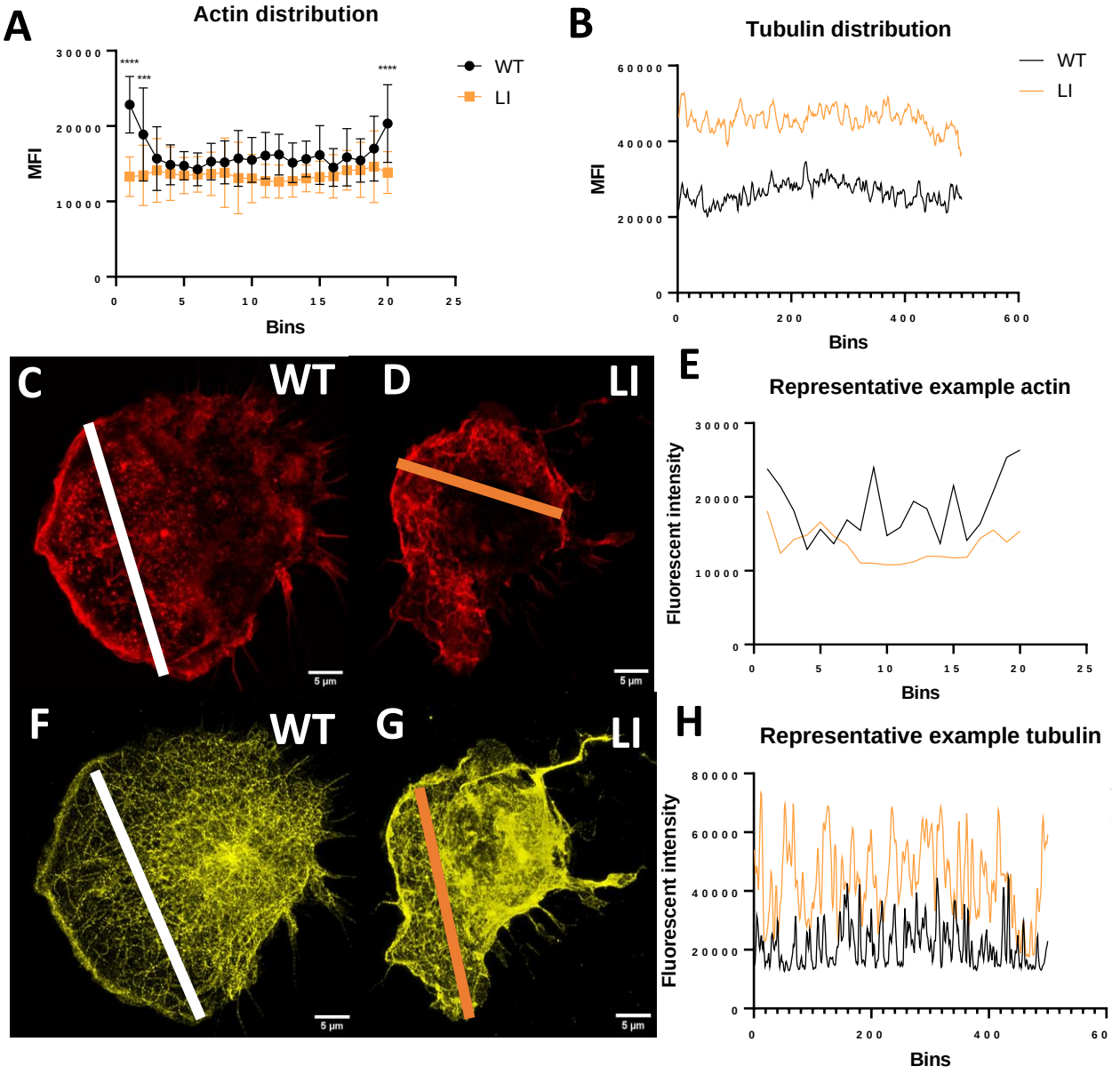

Figure 5: Subcellular actin and tubulin distribution is disrupted in DISC1 LI microglia. An ImageJ macro was used that make a line through the cell and measures the fluorescence intensity over this line; the line is divided into a chosen amount of bins in order to compare cells of all sizes. **(A-B)** The mean fluorescence intensity for each bin was measured for both (A) actin and (B) tubulin. A two-way ANOVA was used to determine the significance. **(C-E)** One representative cell from each genotype was used to compare actin distribution. The bin length of the WT example is 1.9 µm while the LI example has a bin length of 1.1 µm. **(F-H)** One representative example for each genotype was used to compare the tubulin distribution. The bin length of the WT example is 0.077 µm while the LI bin length is 0.060 µm.

fluorescence intensity (MFI) was calculated (Figure 4). WT microglia had a significantly higher actin density (14 744 AU) than DISC1 LI microglia (13 173 AU) ($p = 0.0073$). The tubulin density was significantly higher in the DISC1 LI microglia (25 922 AU) compared to WT microglia (20 027AU) ($p < 0.0001$). These results confirm the observations made from the confocal microscopy images and it indicates that DISC1 plays a crucial

role in maintaining normal actin and tubulin densities.

Next, we wanted to see how the network distribution of actin and tubulin was affected by DISC1 locus impairment. Therefore, we used an analysis tool to measure the intensity over a line that crosses the cell. The line was divided into a predetermined number of bins in order to compare cells of all sizes. Actin distribution has some significant differences between WT and DISC1 LI

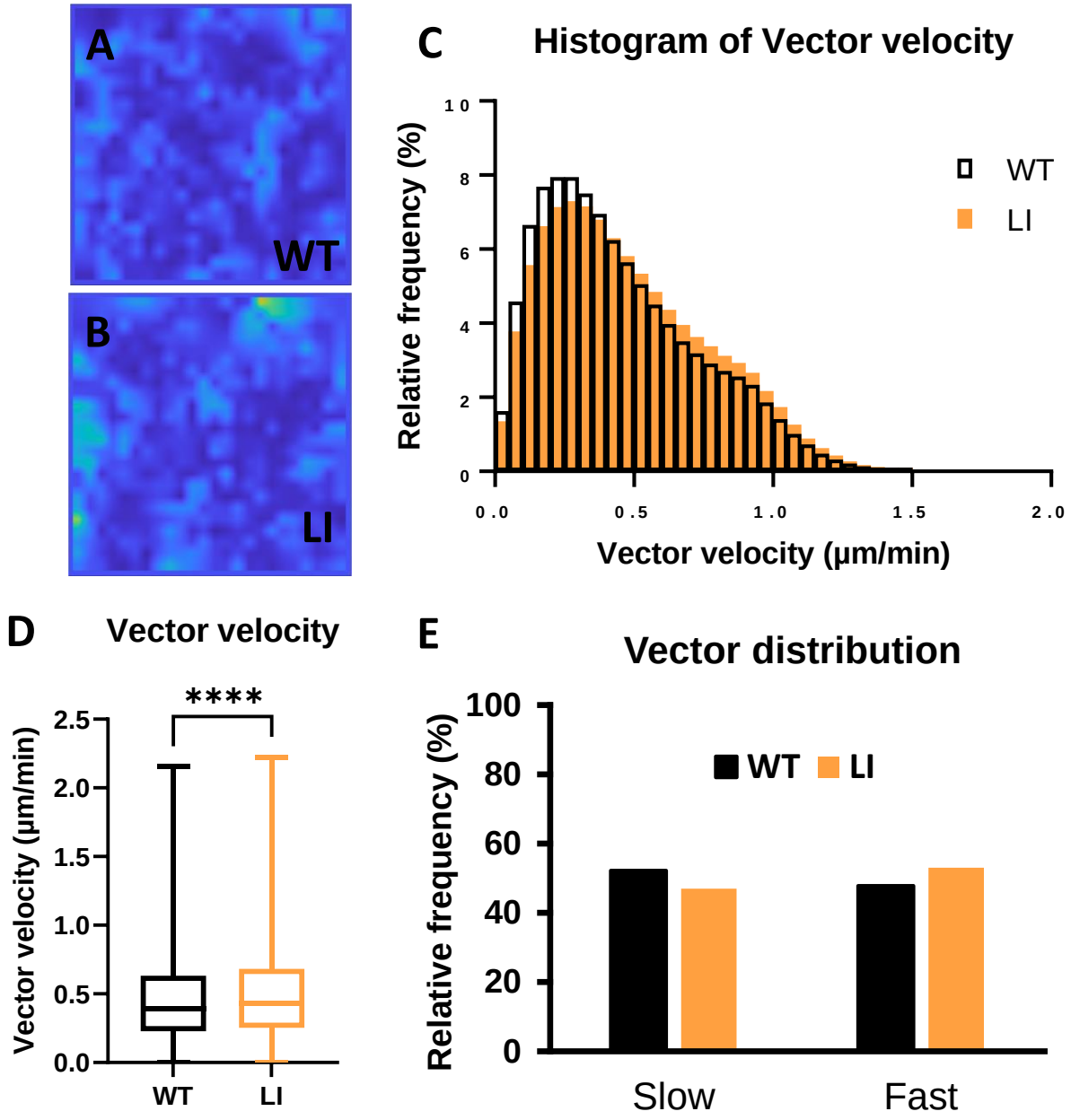

Figure 6: Tubulin dynamics are increased in DISC1 LI microglia. (A-B) Representative heatmaps based on vector velocities of (A) WT and (B) DISC1 LI tubulin in microglia. Scaled from 0 (dark blue) to 2 (yellow) µm/min **(C)** Histogram that includes all vectors obtained from 20 cells per condition (n = 20), each with 20 frames analyzed per cell for a total of 656 641 vectors for each genotype. Bin width is 0.05 µm/min. **(D)** Boxplot showing the distribution of all vectors. Mann-Witney test was performed. **(E)** Bar graph dividing the vectors into two categories: Slow and Fast. The cut-off point is the mean of all vectors (WT+LI). ****p < 0.0001

microglia (Figure 1A). The first 2 bins and the last bin had a significantly higher MFI ($p < 0.001$). These increases in fluorescent intensity are likely to originate from the thick actin border that is seen in WT microglia but not in LI microglia (Figure 3A-D). Overall, the WT actin intensity is higher than LI, confirming the data in Figure 4A. A similar analysis could not determine the individual fibers observed only in the tubulin cytoskeleton of WT microglia but absent in LI microglia. However, the overall fluorescence intensity of tubulin was higher in the LI microglia, something that can also be seen in Figure 4B. Next, we used one representative cell for each genotype to compare the distribution in more detail (Figure 5C-H). The actin distributions (Figure 5E) are similar to the averaged intensity of Figure 5A, although there are some big peaks in the WT distribution. These probably arise from FAs. The tubulin distribution of a representative example (Figure 5H) fluctuates heavily for both the WT and LI microglia. This is due to the high number of bins (500 bins) and the structure of the microtubules. It appears that the fluctuations of the WT microglia are sharper while the LI peaks are generally rounder, suggesting larger tubulin fibers and more densely packed tubulin in LI microglia.

These results indicate that the actin and tubulin distribution and organization are disrupted in DISC1 LI microglia.

Tubulin dynamics are increased in DISC1 LI microglia – So far, we have only investigated the structure of the cytoskeleton of microglia. However, the dynamics of the cytoskeleton are also crucial in understanding the effect of DISC1 on microglial functions. Therefore, we produced SIM images that follow the tubulin structure over time. These images were analyzed in a way that provided us with vectors that describe the speed of the tubulin cytoskeleton from one frame to another. These vectors are represented in a heat map (Figure 6 A-B). The LI heatmap has more activity compared to the WT heatmap, indicating faster tubulin dynamics in LI microglia. Furthermore, all vectors were plotted in a histogram (Figure 6 C), showing the distribution of the vectors for each genotype. The distribution of the LI vectors is shifted towards the right, indicating that the vector speed for tubulin dynamics is higher in LI microglia. This is confirmed in Figure 6D, a boxplot that further summarizes the distribution of the vectors. Here we see that the median (WT = 0.3933 µm/min; LI = 0.4339 µm/min) is significantly higher for the LI microglia ($p < 0.0001$). Finally, we divided all vectors into two categories: slow and fast vectors, with the mean of all vectors as the cut-off point. Here we see that 52.2% of WT vectors are slow, whilst only 47% of LI vectors are classified as slow. These results indicate that tubulin is more dynamic in DISC1 LI microglia compared to their WT counterpart.

DISCUSSION

In his study, we aimed to investigate how DISC1 affects the cytoskeletal organization and dynamics in microglia and, consequently, microglial morphology *in vitro* and *in situ*. The results suggested that DISC1 locus impairment decreases the size of microglia and provides the cells with more aberrant protrusions *in vitro. In situ* experiments, however, showed that LI microglia were more ramified than WT microglia and that this is mostly a microglia-autonomous effect of DISC1. Immunostaining experiments revealed that the actin and the tubulin cytoskeletal organization and density are disrupted in DISC1 LI microglia. The final results showed that the tubulin movement of DISC1 LI microglia was slightly but significantly increased compared to WT microglia. All these results suggest that DISC1 has a significant influence on the cytoskeletal structure, distribution, and dynamics, either direct or indirect, explaining why important cellular activities including migration, ramification, and even phagocytosis are impaired in NDDs.

DISC1 affects microglial morphology – Microglia in their resting state are very ramified in order to scan their environment, while activated microglia are rounded with fewer ramifications. *In vitro* experiments showed that LI microglia were significantly smaller in size and their protrusions deviated from the WT protrusions (Figure 1). WT microglia had lamellipodia 76% of the time, which were only observed in 30% of LI microglia. Lamellipodia are essential for migration, and although filopodia, which are more common in LI microglia, are also important here, they are not necessary for successful cell migration (25). Furthermore, the filopodia are mostly not located on lamellipodia and largely oriented in different directions. This suggests that DISC1 LI microglia are less effective at migrating.

In situ experiments showed that LI microglia were more ramified, even in a DISC1 WT environment (Figure 2). These results were unexpected as microglia in patients with NDD seem to be more active due to a less ramified morphology (43, 44). Furthermore, previously unpublished *in situ* data from the research team of Prof. Brône show that DISC1 LI microglia are less ramified than WT. However, these experiments were performed in full DISC1 WT or LI mice without irradiation, bone marrow transplantation, and CSF1R inhibition. These technical procedures could be an explanation for the discrepancy seen in the outcomes. Moreover, the cells studied in this project are infiltrated microglia-like monocytes that arise from the transplanted bone marrow. Therefore, this is not a perfect model for evaluating the morphology of microglia in the brain. However, it is a model that allows us to determine whether the effect of DISC1 on the morphology of microglia, or microglia-like cells, is due to external signals or the intrinsic DISC1 genotype. We do see that the morphology is mostly dependent on the microglial DISC1 genotype and not on the external environment, however, the level of ramification does not overlap between the same donor types, and there are significant differences among them. This indicates at least some level of external environmental influence on the morphological phenotype. In the CNS, neurons influence microglial activation and thereby, their morphology (45). Moreover, neuronal pathways can be affected by DISC1, so it would be sensible to assume that neuronal signals directed at microglia can be altered in a DISC1 LI environment as well (46).

Furthermore, in this experiment, there was a significant period where no microglia were present in the brain parenchyma. Microglia are essential for maintaining brain homeostasis. Therefore, when the transplanted microglia-like cells arrived, there would have been more activation signals. Although the images were made 13 weeks after the BMT, it could be that it takes longer to return to a new state of brain homeostasis. In that case, it would be logical to see more activated, less ramified microglia. Meanwhile, the LI microglia are more ramified, so this could mean that they cannot be activated effectively in this experiment, and they stay in resting mode even though activation signals are present.

In addition, these transplanted cells need to migrate towards the brain, and DISC1 is known to be important for this process. It could be that only a certain subtype of microglia-like cells reached the brain parenchyma. A type that has the ability to migrate despite DISC1 locus impairment is perhaps more likely to be in a ramified resting state instead of the more classical activated microglia state seen in NDDs.

Cytoskeletal organization and distribution are disrupted in DISC1 LI microglia – A closer look at the microglial cytoskeleton revealed that the actin density was decreased and tubulin density was increased in LI microglia compared to WT microglia (Figure 4). Moreover, the cellular distributions and organization appeared to be altered as well (Figure 5). The density alterations are probably due to a difference in actin or tubulin recruitment and organization that changes the structure and, therefore, the density of the actin and tubulin fibers. However, it must be noted that this could also be because of a difference in the efficiency of the immunostaining, although this is unlikely.

The possible explanation for the actin and tubulin distribution and organization aberrations is that DISC1 has a huge interactome that includes many cytoskeleton-associated proteins. Disrupting DISC1, therefore, affects the cytoskeletal structure. Tubulin-associated proteins, including MIPT3, a cilia-associated protein, and Ndel1, a protein associated with motor proteins dynein and kinesin and microtubule organization, are included in the DISC1 interactome (38, 47). Girdin is an actin-associated protein involved in cytoskeletal remodeling and motility and has been known to form a complex with actin that is essential for actin polymerization in T cells (39). The AKT-mTOR pathway, a large pathway that signals the actin cytoskeleton, can be modulated by DISC1 as well (34). Additionally, other risk genes for neurodevelopmental disorders have been associated with cytoskeletal disorganization in microglia as well, suggesting that cytoskeletal disruption in microglia is present in NDDs (48, 49).

Migration of microglia is essential for proper brain wiring. The disruption of the actin organization in DISC1 LI microglia is crucial in the impairment of microglial migration. The thick ring formation of actin in the lamellipodia is not present in the LI microglia (Figure 3A-D, Figure 5A, C-E).

Instead, there are often irregular-shaped lamellipodia or filopodia that contain the actin instead. This irregularity is not in favor of efficient migration (23). Tubulin is denser and has less structured microtubules (Figure 3E-H, Figure 4B, Figure 5F-H). This density difference could be linked with the smaller size of microglia (Figure 1C). Migration is thought to be more efficient with lower microtubule densities (50), which suggests that the increased tubulin density seen in these results could prove to be important in understanding NDD pathology. Future experiments could focus on migrating cells, using specific migrating assays, and examine the cytoskeletal structure and organization during migration.

Tubulin dynamics are affected by DISC1 – The cytoskeleton is highly dynamic, therefore, we investigated the tubulin dynamics in WT and DISC1 LI microglia. The results showed a significant increase in LI microglial tubulin dynamics compared to WT microglia. These findings are not in line with the expectations as we would expect higher motility in WT microglia because their cytoskeleton is more structured, and we expect them to migrate more efficiently. However, this experiment measures mainly background movement. These movements are not coordinated and do not lead to any cell migration or other meaningful cellular functions. This may be explained by the unstructured actin and tubulin cytoskeleton that is unable to coordinate the movements due to suboptimal cytoskeletal organization or motor protein support. Evidence suggests that microtubules are essential for cell locomotion, and the absence of microtubules makes movement more random (51). This makes it likely that unorganized tubulin, as seen in DISC1 LI microglia, hampers cell locomotion and migration, and increases random movement.

Limitations – This study has provided evidence of DISC1 as a regulator of microglial structure, organization, and movement of the cytoskeleton in mice. However, an animal model does not necessarily represent human pathology. The mouse *Disc1* gene is also significantly different from the human *DISC1* counterpart, however, the function appears to be conserved (52). Next, a BMT model was used to study microglial morphology and the effect of the environment. As mentioned above, this model is not perfect for this purpose. A superior experimental design would include a conditional DISC1 LI model that utilizes the Cre-Lox system in CX3CR1 positive cells. Unfortunately, such a model is not available for DISC1. Other limitations included the imaging quality, as the SIM pictures used for the results in Figure 6 were high in background noise. The noise in the SIM pictures probably did not influence the conclusion of the experiments as we plotted the data in a histogram (Figure 6B) in order to visually filter out the background movement from the real movement, and because all images had the same amount of background. Furthermore, the immunostained cytoskeleton images were supposed to be segmented and analyzed by designated software tools in order to quantify more parameters from these images. However, the DISC1 LI microglia were too aberrated that software packages did not successfully interpret these pictures. Therefore, the line analysis was used, although this method is not ideal as it only takes into account a small portion of the cell. However, it was made sure that the examined part of the cell was representative. Moreover, the actin staining (Phalloidin-Alexa Fluor 647) did not show the classical actin fibers that you expect to see from an actin staining, and a vinculin staining was attempted, but it did not represent the FAs, a crucial component in migration, in a meaningful way.

CONCLUSION

The results in this paper indicate that DISC1 plays an important role in the regulation and organization of the microglial cytoskeleton. This link is crucial evidence for the hypothesis that DISC1, a neurodevelopmental risk gene that is mostly linked to neurons, is associated with microglia in NDDs. Microglia are key players in neurodevelopmental disorders and their cytoskeleton is of the utmost importance for microglial functionality. Therefore, these results could contribute to potential therapeutic targets for NDDs.

REFERENCES

1. Ismail FY, Shapiro BK. What are neurodevelopmental disorders? Curr Opin Neurol. 2019;32(4):611-6.
2. Owen MJ, O'Donovan MC, Thapar A, Craddock N. Neurodevelopmental hypothesis of schizophrenia. Br J Psychiatry. 2011;198(3):173-5.
3. Kloiber S, Rosenblat JD, Husain MI, Ortiz A, Berk M, Quevedo J, et al. Neurodevelopmental pathways in bipolar disorder. Neurosci Biobehav Rev. 2020;112:213-26.
4. Jonsson U, Alaie I, Löfgren Wilteus A, Zander E, Marschik PB, Coghill D, et al. Annual Research Review: Quality of life and childhood mental and behavioural disorders - a critical review of the research. J Child Psychol Psychiatry. 2017;58(4):439-69.
5. Parenti I, Rabaneda LG, Schoen H, Novarino G. Neurodevelopmental Disorders: From Genetics to Functional Pathways. Trends Neurosci. 2020;43(8):608-21.
6. Winden KD, Ebrahimi-Fakhari D, Sahin M. Abnormal mTOR Activation in Autism. Annu Rev Neurosci. 2018;41:1-23.
7. Bădescu GM, Fîlfan M, Sandu RE, Surugiu R, Ciobanu O, Popa-Wagner A. Molecular mechanisms underlying neurodevelopmental disorders, ADHD and autism. Rom J Morphol Embryol. 2016;57(2):361-6.
8. Baird AL, Coogan AN, Siddiqui A, Donev RM, Thome J. Adult attention-deficit hyperactivity disorder is associated with alterations in circadian rhythms at the behavioural, endocrine and molecular levels. Mol Psychiatry. 2012;17(10):988-95.
9. Tang X, Jaenisch R, Sur M. The role of GABAergic signalling in neurodevelopmental disorders. Nat Rev Neurosci. 2021;22(5):290-307.
10. Estes ML, McAllister AK. Maternal immune activation: Implications for neuropsychiatric disorders. Science. 2016;353(6301):772-7.
11. Knuesel I, Chicha L, Britschgi M, Schobel SA, Bodmer M, Hellings JA, et al. Maternal immune activation and abnormal brain development across CNS disorders. Nat Rev Neurol. 2014;10(11):643-60.
12. Han VX, Patel S, Jones HF, Dale RC. Maternal immune activation and neuroinflammation in human neurodevelopmental disorders. Nat Rev Neurol. 2021;17(9):564-79.
13. Jiang HY, Xu LL, Shao L, Xia RM, Yu ZH, Ling ZX, et al. Maternal infection during pregnancy and risk of autism spectrum disorders: A systematic review and meta-analysis. Brain Behav Immun. 2016;58:165-72.
14. Tang D, Kang R, Coyne CB, Zeh HJ, Lotze MT. PAMPs and DAMPs: signal 0s that spur autophagy and immunity. Immunol Rev. 2012;249(1):158-75.
15. Smith SE, Li J, Garbett K, Mirnics K, Patterson PH. Maternal immune activation alters fetal brain development through interleukin-6. J Neurosci. 2007;27(40):10695-702.
16. Ransohoff RM, Cardona AE. The myeloid cells of the central nervous system parenchyma. Nature. 2010;468(7321):253-62.
17. Ginhoux F, Prinz M. Origin of microglia: current concepts and past controversies. Cold Spring Harb Perspect Biol. 2015;7(8):a020537.
18. Smolders SM, Kessels S, Vangansewinkel T, Rigo JM, Legendre P, Brône B. Microglia: Brain cells on the move. Prog Neurobiol. 2019;178:101612.
19. Lenz KM, Nelson LH. Microglia and Beyond: Innate Immune Cells As Regulators of Brain Development and Behavioral Function. Front Immunol. 2018;9:698.
20. Coomey R, Stowell R, Majewska A, Tropea D. The Role of Microglia in Neurodevelopmental Disorders and their Therapeutics. Curr Top Med Chem. 2020;20(4):272-6.

21. Xu ZX, Kim GH, Tan JW, Riso AE, Sun Y, Xu EY, et al. Elevated protein synthesis in microglia causes autism-like synaptic and behavioral aberrations. Nat Commun. 2020;11(1):1797.
22. Sellgren CM, Gracias J, Watmuff B, Biag JD, Thanos JM, Whittredge PB, et al. Increased synapse elimination by microglia in schizophrenia patient-derived models of synaptic pruning. Nat Neurosci. 2019;22(3):374-85.
23. Seetharaman S, Etienne-Manneville S. Cytoskeletal Crosstalk in Cell Migration. Trends Cell Biol. 2020;30(9):720-35.
24. Goodson HV, Jonasson EM. Microtubules and Microtubule-Associated Proteins. Cold Spring Harb Perspect Biol. 2018;10(6).
25. Mishra YG, Manavathi B. Focal adhesion dynamics in cellular function and disease. Cell Signal. 2021;85:110046.
26. Mattila PK, Lappalainen P. Filopodia: molecular architecture and cellular functions. Nat Rev Mol Cell Biol. 2008;9(6):446-54.
27. Sawamura N, Sawa A. Disrupted-in-schizophrenia-1 (DISC1): a key susceptibility factor for major mental illnesses. Ann N Y Acad Sci. 2006;1086:126-33.
28. Millar JK, Christie S, Anderson S, Lawson D, Hsiao-Wei Loh D, Devon RS, et al. Genomic structure and localisation within a linkage hotspot of Disrupted In Schizophrenia 1, a gene disrupted by a translocation segregating with schizophrenia. Mol Psychiatry. 2001;6(2):173-8.
29. Soares DC, Carlyle BC, Bradshaw NJ, Porteous DJ. DISC1: Structure, Function, and Therapeutic Potential for Major Mental Illness. ACS Chem Neurosci. 2011;2(11):609-32.
30. UniProt: the universal protein knowledgebase in 2021. Nucleic Acids Res. 2021;49(D1):D480-d9.
31. Meyer KD, Morris JA. Immunohistochemical analysis of Disc1 expression in the developing and adult hippocampus. Gene Expr Patterns. 2008;8(7-8):494-501.
32. Shevelkin AV, Terrillion CE, Hasegawa Y, Mychko OA, Jouroukhin Y, Sawa A, et al. Astrocyte DISC1 contributes to cognitive function in a brain region-dependent manner. Hum Mol Genet. 2020;29(17):2936-50.
33. Zhou M, Li W, Huang S, Song J, Kim JY, Tian X, et al. mTOR Inhibition ameliorates cognitive and affective deficits caused by Disc1 knockdown in adult-born dentate granule neurons. Neuron. 2013;77(4):647-54.
34. Kim JY, Duan X, Liu CY, Jang MH, Guo JU, Pow-anpongkul N, et al. DISC1 regulates new neuron development in the adult brain via modulation of AKT-mTOR signaling through KIAA1212. Neuron. 2009;63(6):761-73.
35. Srikanth P, Lagomarsino VN, Muratore CR, Ryu SC, He A, Taylor WM, et al. Shared effects of DISC1 disruption and elevated WNT signaling in human cerebral organoids. Transl Psychiatry. 2018;8(1):77.
36. Brandon NJ. Dissecting DISC1 function through protein-protein interactions. Biochem Soc Trans. 2007;35(Pt 5):1283-6.
37. Devine MJ, Norkett R, Kittler JT. DISC1 is a coordinator of intracellular trafficking to shape neuronal development and connectivity. J Physiol. 2016;594(19):5459-69.
38. Wang Q, Brandon NJ. Regulation of the cytoskeleton by Disrupted-in-schizophrenia 1 (DISC1). Mol Cell Neurosci. 2011;48(4):359-64.
39. Maskalenko N, Nath S, Ramakrishnan A, Anikeeva N, Sykulev Y, Poenie M. The DISC1-Girdin complex - a missing link in signaling to the T cell cytoskeleton. J Cell Sci. 2020;133(13).

40. Seshadri S, Faust T, Ishizuka K, Delevich K, Chung Y, Kim SH, et al. Interneuronal DISC1 regulates NRG1-ErbB4 signalling and excitatory-inhibitory synapse formation in the mature cortex. Nat Commun. 2015;6:10118.
41. Zonderland J, Wieringa P, Moroni L. A quantitative method to analyse F-actin distribution in cells. MethodsX. 2019;6:2562-9.
42. Thielicke W, Stamhuis EJ. PIVlab – Towards User-friendly, Affordable and Accurate Digital Particle Image Velocimetry in MATLAB. Journal of Open Research Software. 2014;2.
43. Morgan JT, Chana G, Pardo CA, Achim C, Semendeferi K, Buckwalter J, et al. Microglial activation and increased microglial density observed in the dorsolateral prefrontal cortex in autism. Biol Psychiatry. 2010;68(4):368-76.
44. Zengeler KE, Lukens JR. Innate immunity at the crossroads of healthy brain maturation and neurodevelopmental disorders. Nat Rev Immunol. 2021;21(7):454-68.
45. Wu Q, Li Y, Xiao B. DISC1-related signaling pathways in adult neurogenesis of the hippocampus. Gene. 2013;518(2):223-30.
46. Hansen DV, Hanson JE, Sheng M. Microglia in Alzheimer's disease. J Cell Biol. 2018;217(2):459-72.
47. Steinecke A, Gampe C, Nitzsche F, Bolz J. DISC1 knockdown impairs the tangential migration of cortical interneurons by affecting the actin cytoskeleton. Front Cell Neurosci. 2014;8:190.
48. Muñoz-Estrada J, Lora-Castellanos A, Meza I, Alarcón Elizalde S, Benítez-King G. Primary cilia formation is diminished in schizophrenia and bipolar disorder: A possible marker for these psychiatric diseases. Schizophr Res. 2018;195:412-20.
49. Drew J, Arancibia-Carcamo IL, Jolivet R, Lopez-Domenech G, Attwell D, Kittler JT. Control of microglial dynamics by Arp2/3 and the autism and schizophrenia-associated protein Cyfip1. bioRxiv. 2020:2020.05.31.124941.
50. Bernier LP, Bohlen CJ, York EM, Choi HB, Kamyabi A, Dissing-Olesen L, et al. Nanoscale Surveillance of the Brain by Microglia via cAMP-Regulated Filopodia. Cell Rep. 2019;27(10):2895-908.e4.
51. Fanarraga ML, Villegas JC, Carranza G, Castaño R, Zabala JC. Tubulin cofactor B regulates microtubule densities during microglia transition to the reactive states. Exp Cell Res. 2009;315(3):535-41.
52. Ganguly A, Yang H, Sharma R, Patel KD, Cabral F. The role of microtubules and their dynamics in cell migration. J Biol Chem. 2012;287(52):43359-69.
53. Johnstone M, Thomson PA, Hall J, McIntosh AM, Lawrie SM, Porteous DJ. DISC1 in schizophrenia: genetic mouse models and human genomic imaging. Schizophr Bull. 2011;37(1):14-20.

Acknowledgements – AJ is grateful for the opportunity to follow his internship in the group of Prof. Hendrix. Keerthana Ramanathan is thanked for her guidance and assistance during the internship. Sofie Kessels is sincerely thanked for her assistance, advice, feedback, and helpful explanations. Yeranddy Aguiar Alpizar is thanked for his assistance with data analysis. Sam Duwé is thanked for microscopy introductions and assistance.

Author contributions – KR, JH, and SK conceived and designed the research. AJ, SK, and KR performed experiments, and AJ analyzed the data. AJ wrote the manuscript. All authors carefully edited the manuscript.

Supplementary Figures

Table 1: p- values associated with sholl analysis intersections: All p-values not represented in this table are not significant (p<0,05).

6 µm	WT-WT	LI-LI	WT-LI		**8 µm**	WT-WT	LI-LI	WT-LI
WT-WT	/				WT-WT	/		
LI-LI		/			LI-LI		/	
WT-LI			/		WT-LI			/
LI-WT					LI-WT			
10 µm	WT-WT	LI-LI	WT-LI		**12 µm**	WT-WT	LI-LI	WT-LI
WT-WT	/				WT-WT	/		
LI-LI		/			LI-LI		/	
WT-LI			/		WT-LI			/
LI-WT					LI-WT			
14 µm	WT-WT	LI-LI	WT-LI		**16 µm**	WT-WT	LI-LI	WT-LI
WT-WT	/				WT-WT	/		
LI-LI		/			LI-LI		/	
WT-LI			/		WT-LI			/
LI-WT					LI-WT			
18 µm	WT-WT	LI-LI	WT-LI		**20 µm**	WT-WT	LI-LI	WT-LI
WT-WT	/				WT-WT	/		
LI-LI		/			LI-LI		/	
WT-LI			/		WT-LI			/
LI-WT					LI-WT			
22 µm	WT-WT	LI-LI	WT-LI		**24 µm**	WT-WT	LI-LI	WT-LI
WT-WT	/				WT-WT	/		
LI-LI		/			LI-LI		/	
WT-LI			/		WT-LI			/
LI-WT					LI-WT			
26 µm	WT-WT	LI-LI	WT-LI		**28 µm**	WT-WT	LI-LI	WT-LI
WT-WT	/				WT-WT	/		
LI-LI		/			LI-LI		/	
WT-LI			/		WT-LI			/
LI-WT					LI-WT			
30 µm	WT-WT	LI-LI	WT-LI		**32 µm**	WT-WT	LI-LI	WT-LI
WT-WT	/				WT-WT	/		

LI-LI		/			LI-LI		/	
WT-LI			/		WT-LI			/
LI-WT					LI-WT			
34 µm	WT-WT	LI-LI	WT-LI		**LEGEND:**			
WT-WT	/				NS			
LI-LI		/			p<0.05			
WT-LI			/		p<0.0001			
LI-WT								

Table 2: p-values associated with sholl analysis tips: All p-values not represented in this table are not significant (p<0,05).

6 µm	WT-WT	LI-LI	WT-LI		**8 µm**	WT-WT	LI-LI	WT-LI
WT-WT	/				WT-WT	/		
LI-LI		/			LI-LI		/	
WT-LI			/		WT-LI			/
LI-WT					LI-WT			
10 µm	WT-WT	LI-LI	WT-LI		**12 µm**	WT-WT	LI-LI	WT-LI
WT-WT	/				WT-WT	/		
LI-LI		/			LI-LI		/	
WT-LI			/		WT-LI			/
LI-WT					LI-WT			
14 µm	WT-WT	LI-LI	WT-LI		**16 µm**	WT-WT	LI-LI	WT-LI
WT-WT	/				WT-WT	/		
LI-LI		/			LI-LI		/	
WT-LI			/		WT-LI			/
LI-WT					LI-WT			
18 µm	WT-WT	LI-LI	WT-LI		**20 µm**	WT-WT	LI-LI	WT-LI
WT-WT	/				WT-WT	/		
LI-LI		/			LI-LI		/	
WT-LI			/		WT-LI			/
LI-WT					LI-WT			
22 µm	WT-WT	LI-LI	WT-LI		**24 µm**	WT-WT	LI-LI	WT-LI
WT-WT	/				WT-WT	/		
LI-LI		/			LI-LI		/	
WT-LI			/		WT-LI			/
LI-WT					LI-WT			

LEGEND:								
NS								
p<0.05								
p<0.0001								